

## MULTIVARIATE ANALYSIS FOR RAPID SCREENING AND PREDICTION OF SOLID-STATE COMPATIBILITY IN PHARMACEUTICAL PREFORMULATION STUDIES—PAVING THE ROAD FOR MACHINE LEARNING<sup>1</sup>

Elena Cvetkovska Bogatinovska<sup>1</sup>, Nikola Geškovski<sup>2</sup>, Gjorgji Petrushevski<sup>3</sup>, Viktor Stefov<sup>4\*</sup>

<sup>1</sup>Research and Development, Alkaloid AD, Blvd. Aleksandar Makedonski 12, 1000 Skopje, N. Macedonia

<sup>2</sup>Institute of Pharmaceutical Technology, Faculty of Pharmacy, Ss. Cyril and Methodius University in Skopje, Mother Teresa 47, 1000 Skopje, N. Macedonia

<sup>3</sup>Quality Control Department, Alkaloid AD, Blvd. Aleksandar Makedonski 12, 1000 Skopje, N. Macedonia

<sup>4</sup>Institute of Chemistry, Faculty of Natural Sciences and Mathematics, Ss. Cyril and Methodius University in Skopje, Arhimedova 5, 1000 Skopje, N. Macedonia

viktorst@pmf.ukim.edu.mk

Multivariate analysis models were developed to evaluate the results obtained from a compatibility study designed for ibuprofen with a large group of different types of excipients, as a possible approach for rapid screening of the incompatibility between the active pharmaceutical ingredient (API) and excipients. The solid-state characterization of the binary mixtures was performed by Fourier transform infrared spectroscopy (FTIR) and differential scanning calorimetry (DSC). Principal component analysis (PCA) and partial least squares-discriminant analysis (PLS-DA) using SIMCA<sup>®</sup> software were applied for evaluation of the experimentally obtained results. The optimal PCA model for the FTIR spectra explains 96.2 % of the variations in the dataset with good statistical indicators ( $R^2X = 0.960$ ,  $Q^2 = 0.900$ ), which was also the case for the PCA model for the DSC curves ( $R^2X = 0.981$ ,  $Q^2 = 0.866$ ). The applied PLS-DA models have shown similar behaviour to the PCA. Moreover, the main spectral variations in the FTIR spectra and the thermal events in the DSC data were attributed the highest variable importance for the projection (VIP) scores in the corresponding VIP plots, confirming the model capability for predicting ibuprofen interactions. Furthermore, the prediction power of the optimal models for FTIR and DSC experimental data was evaluated by the root mean square error of prediction (RMSEP) of 0.10 and 0.16, respectively. The obtained results demonstrated the potential of multivariate statistical analysis as a machine learning-based technique for screening and prediction of ibuprofen-excipients solid-state compatibility in the preformulation phase of the pharmaceutical development of dosage forms.

**Keywords:** interaction; binary mixtures; principal component analysis; partial least squares-discriminant analysis; machine learning

## МУЛТИВАРИЈАНТНА АНАЛИЗА ЗА БРЗ СКРИНИНГ И ПРЕДВИДУВАЊЕ НА КОМПАТИБИЛНОСТА ВО ЦВРСТА СОСТОЈБА ВО ФАРМАЦЕВТСКИТЕ ПРЕДФОРМУЛАЦИСКИ СТУДИИ –ТРАСИРАЊЕ НА ПАТОТ ДО МАШИНСКОТО УЧЕЊЕ–

Беа развиени мултиваријантни модели за анализа на евалуација на резултатите добиени во рамките на претходно дизајнирана студија за компатибилност на ибупрофен со поголема група ексципенти, со цел брз скрининг на компатибилноста на активната супстанција и ексципентите. За карактеризација на бинарните смеси во цврста состојба беа користени инфрацрвената спектроскопија со Фуриеова трансформација (FTIR) и диференцијалната скенирачка

<sup>1</sup> Dedicated on the occasion of the Golden Jubilee of the *Macedonian Journal of Chemistry and Chemical Engineering*

калориметрија (DSC). Анализата на основната компонента (PCA) и дискриминаторната анализа на парцијални најмали квадрати (PLS-DA), со помош на софтверскиот пакет SIMCA<sup>®</sup>, беа применети за евалуација на експериментално добиените резултати. Оптималниот модел на PCA добиен за FTIR-спектрите објаснува 96,2 % од промените во сетот со податоци, со задоволителни статистички параметри ( $R^2X = 0,960$ ,  $Q^2 = 0,900$ ), слично како и моделот на PCA развиен за кривите на DSC ( $R^2X = 0,981$ ,  $Q^2 = 0,866$ ). Применетите PLS-DA модели покажаа слични карактеристики како и соодветните PCA модели. Главните спектрални промени во FTIR-спектрите и термалните ефекти во кривите на DSC се карактеризираат со највисоки вредности за степенот на значајност на променливите (Variable importance for the projection – VIP) во соодветните VIP-графици, што ја потврдува способноста на моделот да ги предвидува интеракциите на ибупрофен. Способноста за предвидување оптимални модели добиени од експерименталните податоци за FTIR и DSC беше евалуирана преку процена на вредноста на квадратниот корен од средната квадратна грешка од предвидувањето, односно RMSEP 0,10 и 0,16, соодветно. Добиењите резултати го потврдуваат потенцијалот на мултиваријантната статистичка анализа како техника базирана на машинското учење за скрининг и предвидување на компатибилноста на ибупрофен и ексципиентите во предформулацискиот фармацевтски развој на дозирани форми.

**Клучни зборови:** интеракција; бинарни смеси; анализа на основната компонента; дискриминаторна анализа на парцијални најмали квадрати; машинско учење

## 1. INTRODUCTION

The compatibility of the active pharmaceutical ingredient (API) with potential excipients is a significant segment of pharmaceutical formulation development. Due to the close contact of the API with one or more excipients in the formulation, any kind of interaction or incompatibility between them might result in a negative impact on the stability, physical, chemical or efficacy attributes of the finished product. Therefore, for a rational selection of excipients, screening of API-excipient compatibility is a key aspect of the formulation development process for ensuring safe and robust product development.<sup>1</sup>

With the purpose of fast and precise evaluation of the API-excipient compatibility, as well as appropriate choice of the excipients, different analytical techniques such as spectroscopic, thermoanalytical, microscopic, diffraction, as well as chromatographic methods are widely applied for API-excipient compatibility testing. Fourier transform infrared spectroscopy, as mid-infrared (MIR) and near-infrared (NIR) spectroscopy, along with Raman spectroscopy<sup>2-4</sup> are known as non-destructive and low-cost techniques giving valuable and fast information about the structure and chemical nature of the sample, and thus the observed structural changes signalling possible incompatibilities.<sup>5</sup> Spectroscopic analysis itself might not be sufficient for obtaining all the relevant data in some cases. Therefore, its combination with additional techniques such as x-ray powder diffraction (XRPD), differential scanning calorimetry (DSC) and thermogravimetry (TG) or their simultaneous

combination as TG-IR and DSC-Raman can be very valuable in such cases.<sup>6</sup>

Besides the great potential and excellent data that can be obtained with the above-mentioned techniques, interpretation of spectroscopic data can be at times really challenging, since some of the spectroscopic bands might be misinterpreted, partially interpreted or even wrongly interpreted. Therefore, the employment of artificial intelligence (AI) and machine learning (ML) based algorithms for statistical analysis of large sets of spectroscopic data can be very useful for obtaining accurate qualitative and quantitative data. Moreover, the introduction of AI, ML and computer-assisted chemistry in drug development has shown a remarkable impact on the success rate in the field of pharmaceutical technology, providing a greater understanding of the data generated during pharmaceutical development.<sup>7</sup>

Multivariate statistical methods of analysis are among the most extensively used machine learning-based methods for the interpretation of large data sets. This should not be surprising due to the fact that in the recent years the U.S. Food & Drug Administration (FDA) and the International Conference on Harmonisation (ICH) have focused extensively on building the quality into pharmaceutical and other manufacturing processes, incorporating the quality by design (QbD) approach throughout.<sup>8</sup> Since critical quality attributes (CQAs), critical material attributes (CMAs) and critical process parameters (CPPs) are essential QbD elements, machine learning is now considered a powerful tool for mapping the CMAs and CPPs as input variables and CQAs as output variables in order to generate high-quality data and ena-

ble more accurate predictions for new samples through the application of optimized and trained models. The QbD approach<sup>9</sup> is often combined with process analytical technology (PAT) strategies<sup>10,11</sup> and multivariate analysis, which are designed to achieve more systematic, enhanced acquisition of process-related data, that is high in volume, variety and velocity of generation.<sup>12</sup> As a result, the utilization of these ML-based algorithms facilitates continual improvement and innovation throughout every aspect of the pharmaceutical product's lifecycle. Furthermore, principal component analysis (PCA) and partial least squares regression analysis (PLS) have been shown as a powerful tool for the needs of pharmaceutical product development. PCA as a dimension reduction method is a vastly used approach for the so-called unsupervised learning with the main aim of detecting underlying relationships or patterns in unlabelled data. Therefore, hidden patterns within complex systems can be successfully identified by AI and ML-based techniques. In this context, an artificial neural network model, developed for a large number of drugs and excipients, has been shown as appropriate for developing a predictive tool for drug-excipient incompatibility.<sup>13</sup> The combined use of PCA and hierarchical cluster analysis (HCA) with TG analysis provided a rapid model for investigation of the compatibility of atenolol with selected excipients,<sup>14</sup> as well as in combination with DSC and TG analysis to study the compatibility of acetazolamide with preferred excipients.<sup>15</sup> Moreover, PLS-DA in combination with attenuated total reflectance (ATR)-FTIR has also been shown as appropriate for quantitative determination and classification of diclofenac sodium content in commercially available tablets.<sup>16</sup> PLS regression analysis combined with FTIR and DSC analysis has been used to quantitatively determine the trends related to magnesium stearate content and stress conditions in binary mixtures of ibuprofen and magnesium stearate, which are responsible for the detected solid-state interaction.<sup>17</sup> Over the past decade, the expansion of NIR spectroscopy combined with multivariate analysis has contributed significantly to pharmaceutical technology improvement,<sup>18</sup> being the most common PAT tool for monitoring different technological processes and properties of the finished pharmaceutical products. PCA and PLS regression analyses have been also used in combination with NIR spectroscopy and laser diffraction analysis in order to develop a new model for rapid particle size analysis of ibuprofen.<sup>19</sup> The multivariate analysis approach has been widely established recently for testing of

compatibility between active pharmaceutical ingredients and excipients, as well as drug-drug compatibility testing.

Ibuprofen is one of the most popular non-steroidal anti-inflammatory drugs (NSAIDs) widely used in the treatment of acute pain and fever, as well as in some chronic conditions. Thanks to its excellent analgesic and anti-inflammatory properties, ibuprofen is used as an active pharmaceutical ingredient in various pharmaceutical dosage forms for oral and topical administration, such as tablets, oral suspensions, and gels. The presence of a carboxylic functional group in its structure makes ibuprofen a highly reactive compound. Therefore, it can easily interact with some of the excipients' functional groups, under certain external conditions. Taking this into consideration, ibuprofen was chosen as a model API in this study. The main goal of this study was to design a compatibility study of ibuprofen with a broad spectrum of different excipients which are commonly used in the formulation of solid and liquid pharmaceutical dosage forms and to test the potential application of multivariate analysis as a tool for evaluation and interpretation of the results obtained during the compatibility studies. Furthermore, an assessment of the potential of the statistical models to predict the compatibility between API and excipients and to successfully detect the variables responsible for the observed interactions has been made.

## 2. MATERIALS AND METHODS

### 2.1. Preparation of the binary mixtures

Binary mixtures of ibuprofen (2-[4-(2-methylpropyl)phenyl]propanoic acid) with the selected excipients were prepared in mass ratio 1:1, simulating the worst-case outcome, and labeled according to Table 1. The prepared binary mixtures were analyzed by FTIR and DSC and were placed in stability chambers, exposed to stress conditions at 25 °C/60 % RH and 40 °C/75 % RH, for 30 days. After this period, the stressed binary mixtures were analyzed by the same analytical techniques. The stressed and unstressed ibuprofen in pure form, as well as the binary mixtures marked from BM1–BM54 (Table 1) were used for building of the initial model, while the binary mixtures marked from BM55–BM60 were used for building of the validation test model.

Table 1

*Unstressed and stressed binary mixtures of ibuprofen with selected excipients*

Binary mixture and its label	Technological process
Ibuprofen	Unstressed – Ibuprofen 0 25 °C/60 % RH – Ibuprofen 25 40 °C/75 % RH – Ibuprofen 40 /
Ibuprofen + Silicon dioxide, colloidal anhydrous	Unstressed binary mixture – BM1 25 °C/60 % RH – BM2 40 °C/75 % RH – BM3 Dry mixing
Ibuprofen + Microcrystalline cellulose	Unstressed binary mixture – BM4 25 °C/60 % RH – BM5 40 °C/75 % RH – BM6 Dry mixing
Ibuprofen + Citric acid monohydrate	Unstressed binary mixture – BM7 25 °C/60 % RH – BM8 40 °C/75 % RH – BM9 Dry mixing
Ibuprofen + Crosscarmellose sodium	Unstressed binary mixture – BM10 25 °C/60 % RH – BM11 40 °C/75 % RH – BM12 Dry mixing
Ibuprofen + Disodium edetate	Unstressed binary mixture – BM13 25 °C/60 % RH – BM14 40 °C/75 % RH – BM15 Dry mixing
Ibuprofen + Emulsion simethicone 30 %	Unstressed binary mixture – BM16 25 °C/60 % RH – BM17 40 °C/75 % RH – BM18 Dry mixing
Ibuprofen + Glycerol	Unstressed binary mixture – BM19 25 °C/60 % RH – BM20 40 °C/75 % RH – BM21 Dry mixing
Ibuprofen + Glyceryl dibehenate	Unstressed binary mixture – BM22 25 °C/60 % RH – BM23 40 °C/75 % RH – BM24 Dry mixing
Ibuprofen + Lactose monohydrate	Unstressed binary mixture – BM25 25 °C/60 % RH – BM26 40 °C/75 % RH – BM27 Dry mixing
Ibuprofen + Magnesium stearate	Unstressed binary mixture – BM28 25 °C/60 % RH – BM29 40 °C/75 % RH – BM30 Dry mixing
Ibuprofen + Sodium chloride	Unstressed binary mixture – BM31 25 °C/60 % RH – BM32 40 °C/75 % RH – BM33 Dry mixing
Ibuprofen + Saccharin sodium salt	Unstressed binary mixture – BM34 25 °C/60 % RH – BM35 40 °C/75 % RH – BM36 Dry mixing
Ibuprofen + Sodium citrate dihydrate	Unstressed binary mixture – BM37 25 °C/60 % RH – BM38 40 °C/75 % RH – BM39 Dry mixing
Ibuprofen + Sorbitol	Unstressed binary mixture – BM40 25 °C/60 % RH – BM41 40 °C/75 % RH – BM42 Dry mixing
Ibuprofen + Maize starch	Unstressed binary mixture – BM43 25 °C/60 % RH – BM44 40 °C/75 % RH – BM45 Dry mixing

Table 1 continue

Ibuprofen + Sucrose	Unstressed binary mixture – BM46	Dry mixing
	25 °C/60 % RH – BM47	
	40 °C/75 % RH – BM48	
Ibuprofen + Xanthan gum	Unstressed binary mixture – BM49	Dry mixing
	25 °C/60 % RH – BM50	
	40 °C/75 % RH – BM51	
Ibuprofen + Sodium hydrogen carbonate	Unstressed binary mixture – BM52	Wet granulation with water
	25 °C/60 % RH – BM53	
	40 °C/75 % RH – BM54	
Ibuprofen + Sodium hydrogen carbonate	Unstressed binary mixture – BM55	Dry mixing
	25 °C/60 % RH – BM56	
	40 °C/75 % RH – BM57	
Ibuprofen + Polysorbate 80	Unstressed binary mixture – BM58	Dry mixing
	25 °C/60 % RH – BM59	
	40 °C/75 % RH – BM60	

\*BM – binary mixture. \*\*RH – relative humidity.

## 2.2. Methods

### 2.2.1. Fourier transform infrared (FTIR) spectroscopy

Varian 660 FTIR spectrometer (Varian Inc., Palo Alto, California, USA) was employed for collection of the FTIR spectra. The attenuated total reflectance (ATR) spectra (resolution 4 cm<sup>-1</sup>, 16 scans per spectrum) were collected by using MIR-Acle ZnSe ATR module (Pike Technologies) low-pressure micrometer clamp, in the mid-infrared region from 4000 to 550 cm<sup>-1</sup>. A background spectrum was collected prior to each sample collection.

### 2.2.2. Differential scanning calorimetry (DSC)

DSC measurements were performed on a NETZSCH DSC 204 F1 Phoenix instrument, in aluminum pans with perforated lid (sample mass ≈ 3 mg), from 25 to 100 °C, with 10 °C/min heating rate, under dynamic nitrogen atmosphere (30 ml/min). Indium standard was used for calibration of the instrument.

### 2.2.3. Multivariate data analysis

PCA and partial least squares-discriminant analysis (PLS-DA) were used to analyze the variations within FTIR spectra and DSC curves and their relation to the possible detected interactions, by using the software SIMCA<sup>®</sup> 17 (Umetrics, Umeå, Sweden). The stressed and unstressed ibuprofen in pure form and the unstressed and stressed binary mixtures were defined as rows (objects), while the wavenumbers of the FTIR spectra and

the temperature points from the DSC temperature range were defined as columns (variables) within the data set. The FTIR spectra and DSC curves were normalized using standard normal variate (SNV) processing and each model was characterized by correlation ( $R^2X$  and  $R^2Y$ ) and predictivity ( $Q^2$ ) coefficients. The score scatter plots and the variable importance of the projection (VIP) plots were used for further evaluation of the models.

## 3. RESULTS AND DISCUSSION

### 3.1. Analysis of unstressed and stressed binary mixtures

#### 3.1.1. Solid-state characterization of the experimental data

The analysis of the obtained FTIR spectra revealed that the observed changes in terms of band shift, intensity, and shape, as well as appearance of new bands, can be generally divided into two groups. Binary mixtures in which no changes were observed, i.e., the binary mixtures that remain stable when exposed to stress conditions, belong to the first group. The second group comprises the cases where some serious changes were observed within the binary mixtures that arise as a result of chemical interactions and the formation of new molecular entities.

Similarly, the presence of the characteristic endothermic peak corresponding to the melting of ibuprofen (maximum temperature 77.7 °C and enthalpy  $\Delta H = 136.9$  J/g) in the DSC curves of the binary mixtures is considered proof of the absence of interactions between the API and corresponding

excipients, and its presence was observed in almost all of the analyzed mixtures. The shift of the endothermic peak of ibuprofen to lower temperatures in some of the binary mixtures, compared to pure ibuprofen melting peak, is expected and justified, keeping in mind that the analyzed samples are physical mixtures of two components, so these, along with the enthalpy changes, are not regarded as interactions.

Based on the presented FTIR and DSC results it can be observed that the increase in temperature and relative humidity most surely leads to an interaction in the binary mixture of ibuprofen and sodium hydrogen carbonate, prepared by dry mixing. In the FTIR spectrum of the mixture exposed to 40 °C/75 % RH (Fig. 1a) the intensity of the band from the carbonyl stretching vibration of ibuprofen at 1710 cm<sup>-1</sup> is significantly decreased and almost lost. This might be an indication of the decreasing quantity of unreacted ibuprofen in the mixture. The appearance of new bands at 1475 cm<sup>-1</sup> and 1406 cm<sup>-1</sup>, resulting from asymmetric and symmetric stretching vibrations of the carboxylate group in the possible structure of the newly formed entity, can be considered an additional indication of the chemical interaction between ibuprofen and sodium hydrogen carbonate forming a new molecular entity.<sup>20,21</sup> Furthermore, the very low intensity band from asymmetric stretching C–O vibrational mode at 1293 cm<sup>-1</sup> appearing for the first time in

the binary mixture exposed to 25 °C/60 % RH, can be identified as a clearly defined new vibrational band with medium intensity in the mixture exposed to 40 °C/75 % RH. This can be attributed to the gradual formation of a new entity, starting at lower humidity and becoming more intensive as the humidity level increases. Moreover, the appearance of new vibrational bands at 1251 cm<sup>-1</sup>, 1057 cm<sup>-1</sup>, 1021 cm<sup>-1</sup> and 942 cm<sup>-1</sup> can be considered as additional confirmation of the interaction taking place between ibuprofen and sodium hydrogen carbonate. In addition, the vibrational band at 865 cm<sup>-1</sup> is lost in the FTIR spectra of the binary mixture exposed to higher temperature and humidity levels. Furthermore, when the same binary mixture was prepared by wet granulation with water, the previously described changes in terms of the appearance of new vibrational bands could be already observed in the unstressed binary mixture (Fig. 1b), implying that this interaction is moisture dependent. This is in good agreement with the disappearance of the endothermic peak of ibuprofen and the appearance of a new endothermic peak at around 85 °C in the corresponding DSC curves (Fig. 3b), attributed to the dehydration process that is known to occur in that temperature range.<sup>22</sup> The same binary mixture, prepared by dry mixing and stressed at 40 °C/75 % RH (Fig. 3a), displayed similar thermal behavior.

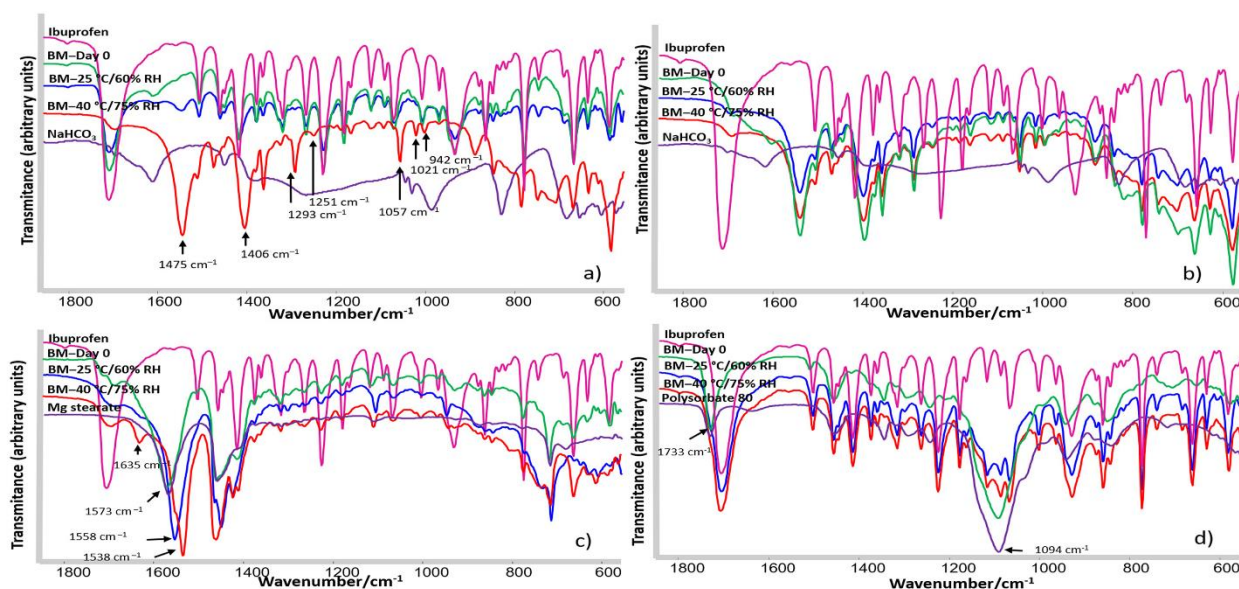


**Fig. 1.** FTIR spectra in the fingerprint region of the unstressed (Day 0) and stressed (Day 30) binary mixture of ibuprofen and sodium hydrogen carbonate prepared by a) dry mixing and b) wet granulation, c) binary mixture of ibuprofen and magnesium stearate and d) ibuprofen and polysorbate 80

The discussed product of interaction is formed as a result of a simple acid-base reaction (Fig. 2). Since ibuprofen contains a carboxylic functional group in its structure, it is considered a weak acid ( $\text{pH} = 4$ ,  $\text{p}K_a = 5.2$ ), while the sodium hydrogen carbonate is a weak base ( $\text{pH} \approx 8.5$ ,  $\text{p}K_b = 10.3$ ,  $\text{p}K_a = 7.7$ ). In the presence of water, during the preparation of the binary mixture, the sodium hydrogen carbonate easily deprotonates the carboxylic group in the ibuprofen molecule, which acts as a proton donor. The sodium hydrogen car-

bonate donates an electron pair from its negatively charged oxygen atom to form a bond with the deprotonated  $\text{CO}_2^-$  group, while at the same time it accepts the proton from the carboxylic group to form carbonic acid. This reaction produces sodium salt of ibuprofen and carbonic acid,  $\text{HOCO}_2\text{H}$ , which is very unstable and readily decomposes to carbon dioxide and water. In presence of the excess of water molecule, as well as the high atmospheric moisture, the obtained sodium salt then quickly converts to its stable dihydrate form.

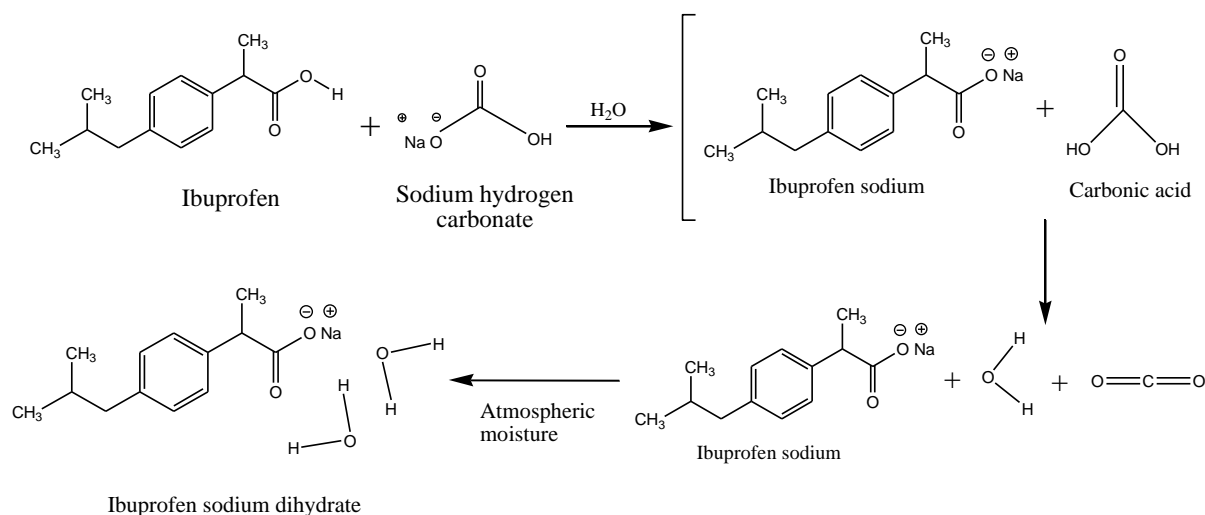


**Fig. 2.** Reaction scheme for the interaction between ibuprofen and sodium hydrogen carbonate

A notable decrease in the intensity of the band from the carbonyl mode of ibuprofen at  $1710\text{ cm}^{-1}$  was also observed in the unstressed and stressed binary mixtures of ibuprofen with the excipient magnesium stearate (Fig. 1c). In line with this observation, the DSC curve of the unstressed binary mixture exhibits an endotherm at around  $58\text{ }^\circ\text{C}$ , while the characteristic endothermic peak of ibuprofen has disappeared (Fig. 3c). This result is in good agreement with the literature data, since the interaction between ibuprofen and magnesium stearate has already been studied and described in the scientific literature.<sup>17</sup> Within this paper, magnesium stearate was included solely for the purpose of building the statistical model for prediction of interactions. Moreover, it can be observed that the band due to the asymmetric stretching carboxylate mode at  $1573\text{ cm}^{-1}$ , originating from magnesium stearate, is shifted to lower frequencies in the FTIR spectra of the stressed binary mixtures and is accompanied by the appearance of new bands at  $1635\text{ cm}^{-1}$  and  $1538\text{ cm}^{-1}$  in the binary mixture stressed at  $40\text{ }^\circ\text{C}/75\text{ \% RH}$  (Fig. 1c). Furthermore,

Stojanovska Pecova et al.<sup>17</sup> showed that the accompanying shift of the characteristic endothermic peak of ibuprofen to lower temperature<sup>23</sup> in the corresponding DSC curve of the unstressed binary mixture is not a result of the simultaneous melting of the eutectic mixture of ibuprofen and magnesium stearate, as it was believed,<sup>24</sup> but is a new endotherm originating from two simultaneous evaporating processes: evaporation of the water from the pseudopolymorphic form of magnesium stearate and evaporation of the water from the in situ-generated diibuprofen magnesium tetrahydrate salt.<sup>17</sup> This was further confirmed by DSC/TG analysis of unstressed and stressed binary mixtures, where the DSC/TG curves of the stressed mixtures exhibited a mass loss in the same temperature range as the endotherms in the DSC curves. Furthermore, the mass loss was shifted to higher temperatures by elevating the stress conditions, implying that the endotherm in the binary mixtures, observed before the ibuprofen melting peak, cannot be attributed to eutectic melting, but is a result of an evaporation process.



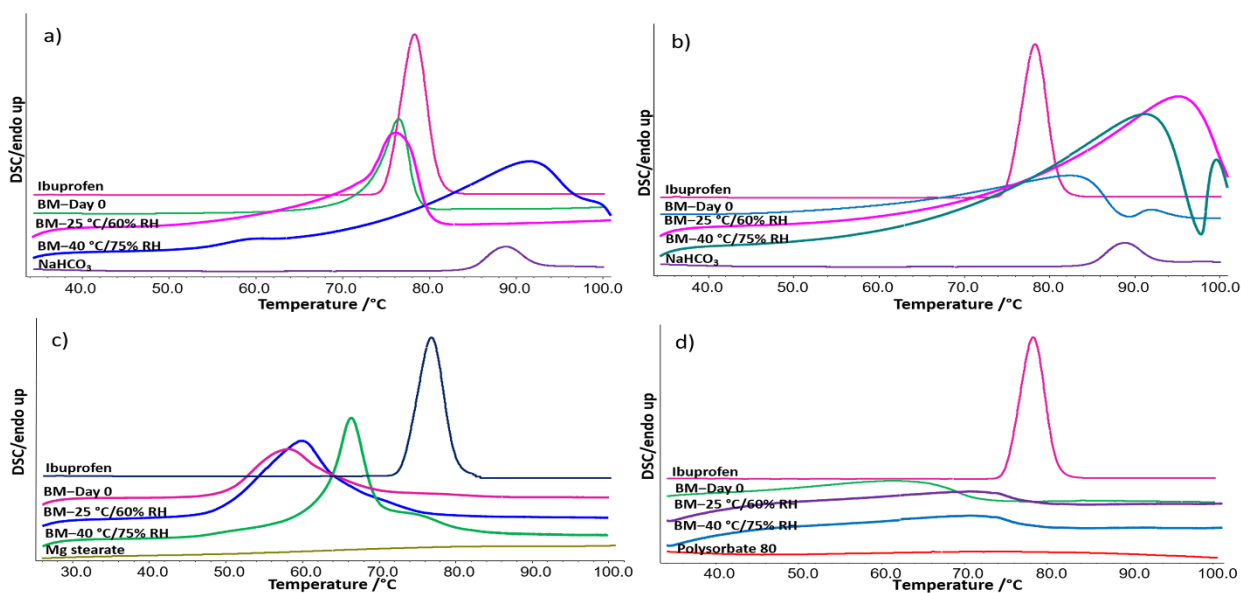


Fig. 3. DSC curves of the unstressed (Day 0) and stressed (Day 30) binary mixture of ibuprofen and sodium hydrogen carbonate prepared by a) dry mixing and b) wet granulation, c) binary mixture of ibuprofen and magnesium stearate and d) ibuprofen and polysorbate 80

While the above-discussed changes unambiguously implied interactions taking place in the binary mixtures, some of the studied mixtures exhibited physical changes which are not considered as interactions. However, their prompt detection is equally important as in some cases they might seriously impact the physicochemical and therapeutic properties of the pharmaceutical formulations. Such behavior was present in the binary mixture of ibuprofen and polysorbate 80 where changes in the FTIR spectra and DSC curves of the unstressed and stressed mixture can be observed. Moreover, the FTIR spectrum of the initial binary mixture is almost identical to the FTIR spectrum of the excipient polysorbate 80 (Fig. 1d). Knowing that the binary mixture was prepared in 1:1 ratio, the unstressed mixture was in liquid state and therefore the appearance of the bands at  $1733\text{ cm}^{-1}$  and  $1094\text{ cm}^{-1}$ , originating from the polysorbate 80, is justified. However, the FTIR spectra of the stressed binary mixtures exhibit vibrational bands originating from both the API and the excipient, which is expected since the viscosity of polysorbate 80 drops at higher temperature levels and thus the API tends to solubilize better in the liquid excipient.<sup>25</sup> This was accompanied by the broadening and simultaneous shifting of the endothermic peak to a lower temperature in the corresponding DSC curve of the unstressed mixture (Fig. 3d), which is justified, since the crystalline structure is also affected under these conditions.<sup>26</sup> This broad melting peak is slightly shifted to higher temperatures, closer to the melting temperature of ibuprofen, in the DSC curves of the stressed binary mixtures. However,

this is not expected to happen during the technological process, since the binary mixture in the preformulation compatibility testing is prepared in 1:1 ratio, which would not be the case in a real formulation where polysorbate 80 is usually added in significantly lower concentrations.<sup>27</sup> On the other hand, the absence of new vibrational bands of unknown origin in the corresponding FTIR spectra of the binary mixture before and after exposure to stress conditions, confirms that the observed behavior of the DSC curve is solely a physical phenomenon and thus no interaction is taking place.

### 3.2. Multivariate data analysis

#### 3.2.1. Principal component analysis (PCA)

##### 3.2.1.1. PCA based on FTIR spectra

The initial PCA was performed on fifty-seven samples of stressed and unstressed ibuprofen in pure form and unstressed and stressed binary mixtures in order to test the possibility of separating and/or grouping the samples based on some mutual spectroscopic features observed in the FTIR spectra. The binary mixtures marked from BM1–BM54, as in Table 1, were used for building the initial model. The optimal PCA model of the SNV-transformed FTIR spectra was built on twelve principal components explaining 96.0 % of the variation in the dataset, with satisfactory statistical indicators ( $R^2X = 0.960$  and  $Q^2 = 0.900$ ). From the presented data (Fig. 4a), it can be observed that the binary mixtures of ibuprofen and sodium hydrogen carbonate, prepared by wet gran-



ulation (BM52, BM53 and BM54) exhibit notable deviation from the general trend of the model. Expectedly, a similar deviation of the model trend can

be observed in the binary mixtures of ibuprofen and magnesium stearate (BM28, BM29 and BM30).

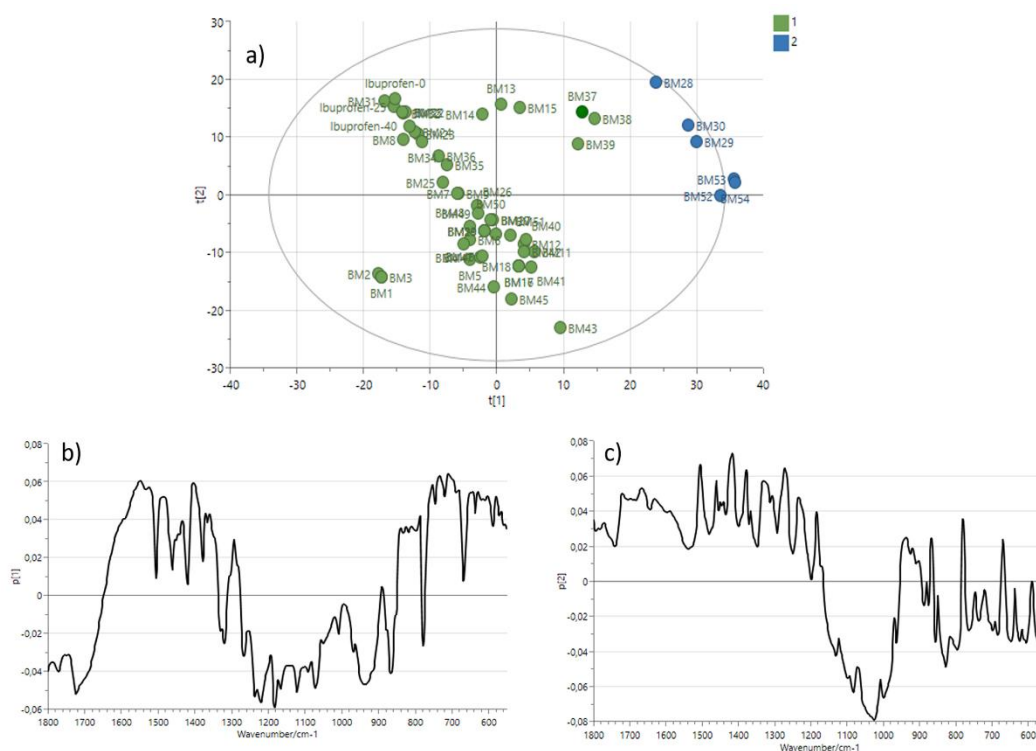


**Fig. 4.** a) Score scatter plot obtained from the PCA model for the FTIR spectra, color based on the type of interaction (green – BMs in which no interaction was detected; blue – BMs in which an interaction was detected) and corresponding loading plots for the b) first and c) second principal component

### 3.2.1.2. PCA based on DSC curves

PCA was performed on the DSC data obtained for the same fifty-seven samples of stressed and unstressed ibuprofen in pure form and unstressed and stressed binary mixtures in order to test the possibility of separating the samples based on some mutual thermal features observed in the DSC curves. The optimal PCA model was built on ten principal components explaining 98.1 % of the variation in the dataset, with satisfactory statistical indicators ( $R^2X = 0.981$  and  $Q^2 = 0.866$ ). Based on the score scatter plot built on the full temperature range of the DSC curves (Fig. 5a), it can be observed that the model groups the samples based on the type of interaction or other type of change, if present. Moreover, it can be observed that the binary mixtures of ibuprofen and sodium hydrogen carbonate prepared by wet granulation (BM52, BM53 and BM54) exhibit notable deviation from the general trend of the model, i.e., they are significantly distanced from the center of the model plane. Similarly, a deviation from the model trend is noticeable in the binary mixtures of ibuprofen

and magnesium stearate, especially in the unstressed mixture (BM28) and the one stressed at 25 °C/60 % RH (BM29).

### 3.2.2. Partial least squares-discriminant analysis (PLS-DA)

PLS-DA models were developed for both FTIR spectra and DSC curves of the stressed and unstressed ibuprofen in pure form and binary mixtures marked from BM1–BM54, as in Table 1. The main criterion for classification of the samples within the model was the prior knowledge of the interactions and their type, from the experimental data. Therefore, all samples were classified into two classes. The binary mixtures in which no interaction was detected were classified as Class 1, while Class 2 comprised the binary mixtures in which an interaction was detected. The final aim of such a designed model was to obtain a low-cost and rapid modulus for evaluation of compatibility between API and excipients, i.e., to obtain a model that would successfully predict interactions and classify other excipients that might be used in fu-

ture formulations of ibuprofen. Furthermore, the prediction power of the optimal models was evaluated in a separate data set using the RMSEP of Y variable (Class). In the context of PLS-DA, the Y variable is assigned a dummy variable ranging

from 0 to 1, representing the two observed classes. Therefore, both, root mean square error of estimation (RMSEE) and RMSEP are calculated as errors in predicting the Y (dummy variable) of the calibration and prediction set, respectively.

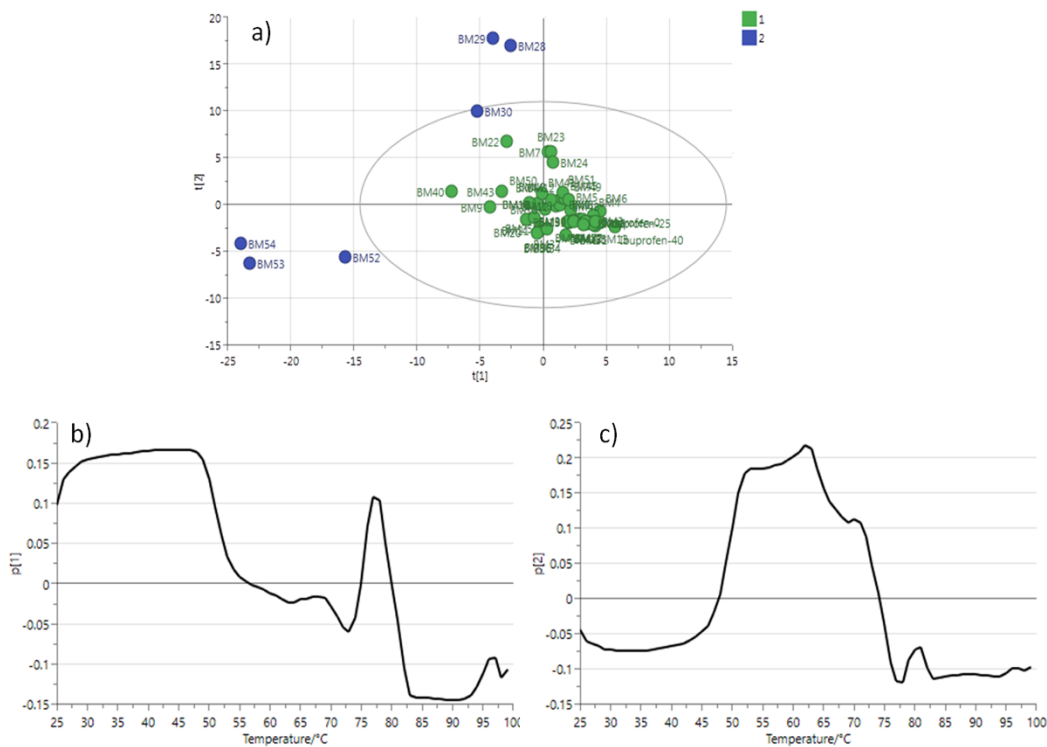


**Fig. 5.** a) Score scatter plot obtained with the PCA model for the DSC curves, color based on the type of the interaction (green – BMs in which no interaction was detected; blue – BMs in which an interaction was detected) and corresponding loading plots for the b) first and c) second principal component

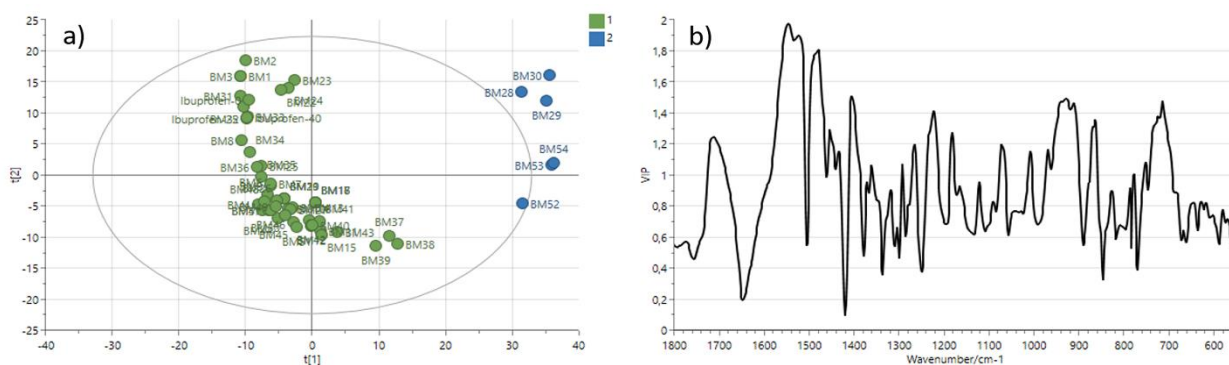


**Fig. 6.** a) Score scatter plot and b) VIP plot of the PLS-DA model for the fingerprint region of the FTIR spectra, color based on the type of the interaction (green – BMs in which no interaction was detected; blue – BMs in which an interaction was detected)

### 3.2.2.1. PLS-DA based on FTIR spectra

The initial PLS-DA model of the SNV-transformed FTIR spectra was built on four PLS factors, characterized by satisfactory correlation factors ( $R^2X = 0.815$  and  $R^2Y = 0.973$ ) and predictivity level ( $Q^2 = 0.946$ ). The fingerprint region

was found to be the best choice for this type of analysis since it encompasses more features based on which the separation and classification can be done with better certainty and correlation. The score scatter plot (Fig. 6a) indicates that the samples are classified and separated based on the type of interaction, similar to the data obtained with

PCA. The variable importance of the projection, or the VIP plot (Fig. 6b), depicts the spectral regions which are directly affected by the stress conditions and are at the same time responsible for the variances in the model, such as changes in the vibrational bands' intensity and position and appearance of new vibrational bands.

### 3.2.2.2. PLS-DA based on DSC curves

The PLS-DA model of the original DSC curves was built on four PLS factors, characterized by satisfactory correlation factors ( $R^2X = 0.855$  and  $R^2Y = 0.889$ ) and lower predictivity level ( $Q^2 =$

0.799). This model behavior can be explained since the DSC curves exhibit very limited features such as the melting peak of ibuprofen, and eventual water evaporation from absorbed moisture or crystalline water evaporation. The score scatter plot (Fig. 7a) indicates that the samples are classified and separated based on the type of interaction, similar to the data obtained with PCA. The VIP plot (Fig. 7b) clearly depicts the temperature regions featuring these DSC events which are directly affected by the stress conditions and are considered as main variances responsible for the model behavior.

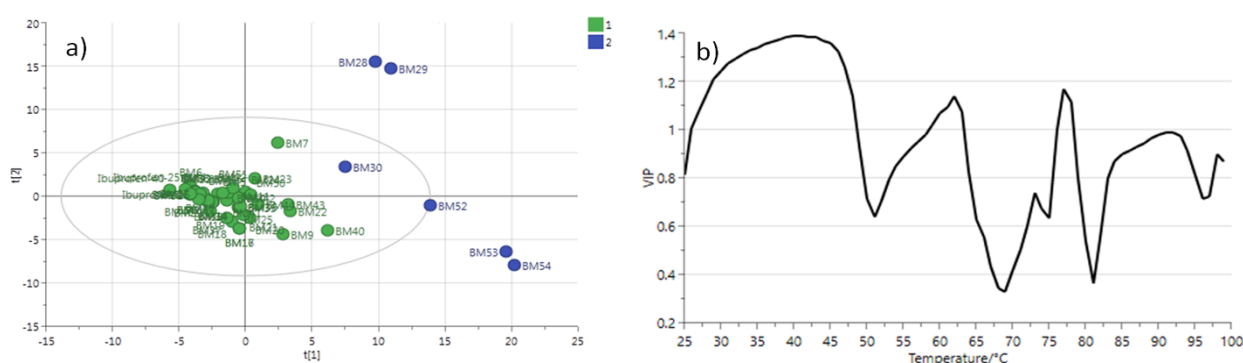


**Fig. 7.** a) Score scatter plot and b) VIP plot of the PLS-DA model for the DSC curves, color based on the type of the interaction (green – BMs in which no interaction was detected; blue – BMs in which an interaction was detected)

### 3.2.3. Testing of the predictive power of PLS-DA models

Several additional binary mixtures were used as a separate training set to evaluate the predictive power of the optimized models to predict new interactions between API and other excipients that might be used in the future formulations of ibuprofen. The prediction training set consisted of the unstressed and stressed binary mixtures of ibuprofen and sodium hydrogen carbonate, prepared by dry mixing (BM55, BM56 and BM57), as well as the binary mixtures of ibuprofen and polysorbate 80 (BM58, BM59 and BM60). Since the interaction between ibuprofen and sodium hydrogen carbonate is moisture dependent, it occurs at more severe stress conditions (40 °C/75 % RH) when the mixture is prepared by dry mixing. On the other hand, the interaction does not occur in the unstressed mixture, while its exposure to milder

stress conditions (25 °C/60 % RH) leads to some subtle changes in the FTIR spectra and DSC curves. This is an adequate choice for model testing since it encompasses examples of both groups of mixtures – the ones in which interaction is detected and the ones in which no interaction is detected. On the other hand, the binary mixture with polysorbate 80 presents a case where no interaction is detected, but the observed changes are attributed to the excipient's properties resulting in some changes between the FTIR spectra of the unstressed and stressed mixtures, as well as physical changes in the DSC curves. The obtained results from the prediction set used for the evaluation of the predictive power of the models for FTIR and DSC data are presented in Figure 8. The obtained RMSEP was 0.10 and 0.16 for the optimal FTIR and DSC models, respectively, and the rate for correct prediction was 100 % for both models.

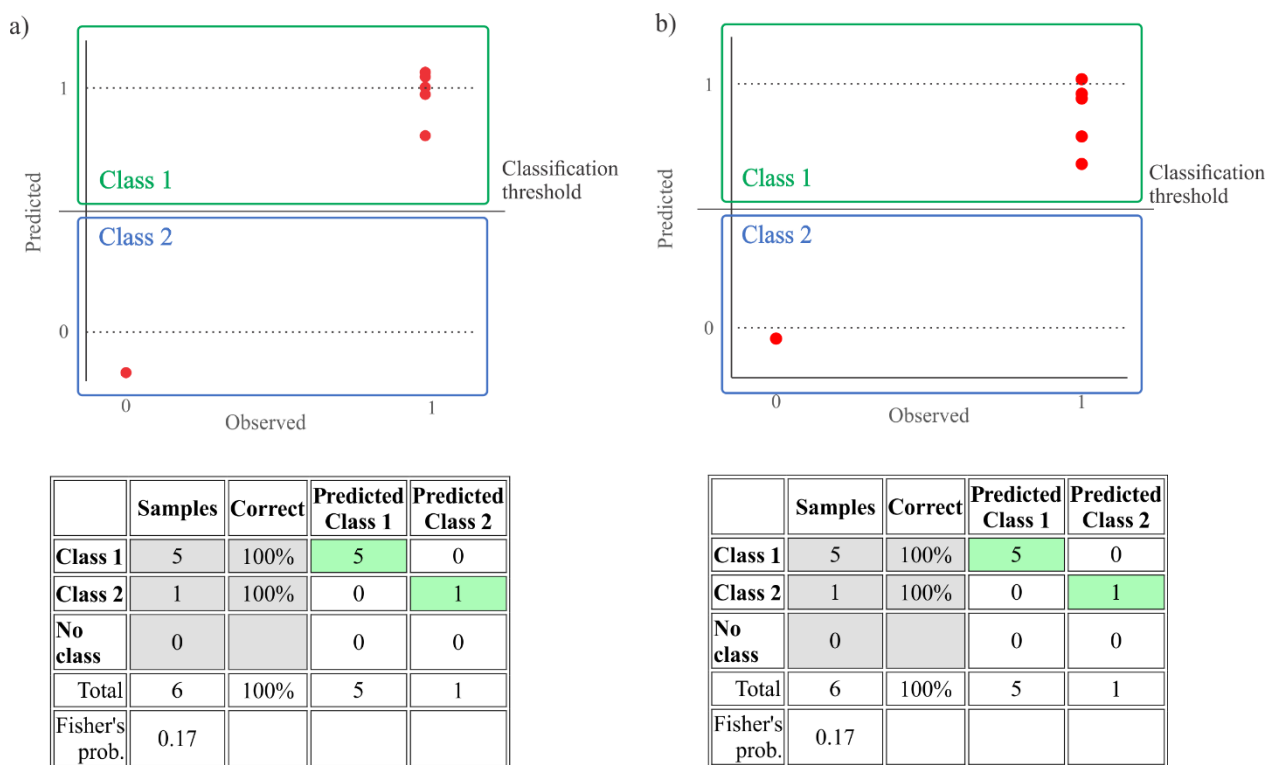


**Fig. 8.** Observed versus predicted plot and the appropriate misclassification table for the prediction set of the a) FTIR spectra model and b) DSC curves model. The green and blue rectangles represent the boundary area for the appropriate class affiliation.

### 3.2.4. Multivariate statistical analysis

The results obtained with the applied statistical models were in accordance with the described experimental data. Keeping in mind that the vibrational bands in the FTIR spectra of the studied binary mixtures originate mainly from ibuprofen, their grouping is based on the bands exhibiting the same or similar wavenumbers, so any major deviation from this trend would be unambiguously detected. Similar approaches have been reported in the literature.<sup>28</sup> According to this observation, if we look more thoroughly at the rest of the binary mixtures in the score scatter plot of the optimal PCA model built for the FTIR spectra (Fig. 4a) it can be seen that most of them are grouped together near the center of the model plane. These are the binary mixtures in which the main vibrational bands originate from ibuprofen and remain unchanged after exposure to stress conditions. On the other hand, minor subgroups can be perceived as well, placed on opposite sides of the plane. The one subgroup consists of the binary mixtures of ibuprofen and sodium citrate dihydrate (BM37, BM38 and BM39) and this observation can be attributed to the fact that this binary mixture exhibits some strong vibrational bands originating from the excipient along with those from the API. Conversely, the

other subgroup consists of the binary mixtures of ibuprofen and colloidal, anhydrous silicon dioxide (BM1, BM2 and BM3) and this observation can be attributed to the fact that some of the most intense vibrational bands in this binary mixture are due to the excipient, not the API. This is expected considering that the excipient is a very light and bulky powder that prevents agglomeration by coating the API particles.<sup>29</sup> However, these binary mixtures are part of the large group of mixtures in which no interaction was detected. Based on the corresponding loading plots (Fig. 4b and 4c) it can be observed that the first principal component classifies the samples according to the main changes in the FTIR spectra, i.e., the changes in the region of carbonyl and carboxylate vibrational mode, as well as the appearance of the previously discussed new bands. The second component classifies the samples according to the presence of some vibrational bands originating from some of the excipients, which might lead to observable changes in the corresponding FTIR spectra. Moreover, it can be concluded that the changes accompanied by the appearance of new bands attributed to the formation of new entities have opposite values and are clearly separated from the ones that are attributed to physical changes manifested as changes in bands' intensity or appearance of bands originating from the

excipients. This confirms the ability of the model to differentiate the interactions or changes based on their different origin.

Similarly, the optimal PCA model built for the DSC curves groups the samples based on some mutual thermal features observed in the DSC curves.<sup>30</sup> The corresponding loading plots (Fig. 5b and 5c) reveal that the model groups based on the main changes in the DSC curves, i.e., the changes in the melting peak of ibuprofen, such as its shift towards higher temperature, as well as changes in its symmetry or enthalpy, was already discussed previously. Moreover, it can be observed that the first principal component classifies the samples according to the shifting of the melting peak of ibuprofen towards higher temperature (Fig. 5b), while the second principal component classifies the samples according to the shifting of the melting peak of ibuprofen towards lower temperature (Fig. 5c).

The corresponding VIP plots from the PLS-DA models reveal the main variances in the FTIR spectra and DSC events in the DSC curves attributable to the API-excipient interactions. The VIP plot (Fig. 6b) for the PLS-DA model built for the FTIR spectra depicts the spectral regions which are directly affected by the stress conditions and are at the same time responsible for the variances in the model, such as changes in the vibrational bands' intensity and position and the appearance of new vibrational bands. The decrease of the intensity of the vibrational band at  $1710\text{ cm}^{-1}$ , as well as the appearance of new vibrational bands at  $1475\text{ cm}^{-1}$ ,  $1406\text{ cm}^{-1}$ ,  $1293\text{ cm}^{-1}$  and  $1251\text{ cm}^{-1}$  in the binary mixture of ibuprofen and sodium hydrogen carbonate prepared by wet granulation (BM52, BM53, BM54), are assigned the highest VIP scores and are related to the new entity formation in the binary mixtures of ibuprofen and sodium hydrogen carbonate. In addition, the shift of the vibrational band at  $1573\text{ cm}^{-1}$  in the binary mixture of ibuprofen and magnesium stearate (BM28, BM29, BM30) and the appearance of new bands at  $1635\text{ cm}^{-1}$  and  $1538\text{ cm}^{-1}$  are also associated with high VIP scores and can be related to the asymmetric and symmetric stretching vibrations of the carboxylate mode.

On the other hand, the characteristic melting peak of ibuprofen around  $77\text{ }^{\circ}\text{C}$  is associated with high VIP score in the corresponding VIP plot (Fig. 7b) since it is the main DSC event in the DSC curves and it features all of the binary mixtures in which the same pattern is present, and thus no interaction was detected. The high VIP score at  $81\text{ }^{\circ}\text{C}$  is attributed to the loss of the ibuprofen melting peak and the appearance of a new endothermic

process at  $\approx 85\text{ }^{\circ}\text{C}$  in the binary mixture of ibuprofen and sodium hydrogen carbonate (BM52, BM53 and BM54), prepared by wet granulation. In addition, the appearance of a new endothermic peak at  $58\text{ }^{\circ}\text{C}$  in the unstressed binary mixture of ibuprofen and magnesium stearate (BM28) is given with a high VIP score as well and is likely related to the appearance of a new endothermic peak featuring two simultaneous evaporating processes occurring in previously discussed formation of the generated magnesium salt of ibuprofen. These data are in good correlation with the data obtained with PCA, and therefore it can quite satisfactorily predict deviations in larger data sets.

The predictive power<sup>31</sup> of the optimized models was further confirmed by testing a separate prediction training sets of binary mixtures for both models for FTIR and DSC. Based on the highest VIP scores explaining the main spectral variations and thermal events in the presented FTIR and DSC data, the model should predict if an interaction is occurring within a binary mixture and classify its type in the appropriate group or subgroup in the score scatter plot. The presented results for the prediction set of the FTIR spectra and DSC curve models clearly depict that the model can predict the interaction in the stressed binary mixture of ibuprofen and sodium hydrogen carbonate, prepared by dry mixing (BM57), and therefore classify this mixture in the group of mixtures in which interactions were detected. On the other hand, unstressed binary mixture (BM55) and the one stressed at milder stress conditions (BM56) are classified in the group of mixtures in which no interaction was detected. Similarly, the binary mixtures of ibuprofen and polysorbate 80 (BM58, BM59 and BM60) are also classified within this group. Furthermore, it can be confirmed that the classification of the mixtures used as a prediction set is in correlation with the above-described grouping and observations.

#### 4. CONCLUSION

The applied solid-state techniques in combination with multivariate analysis were found to be appropriate for API-excipient compatibility studies and prediction of potential interactions. The statistical models provided satisfactory statistical indicators and have quite satisfactorily separated the analyzed binary mixtures based on the interaction type. As a result, the binary mixtures in which strong interactions were detected were successfully differentiated from the binary mixtures in which interactions were not detected. Furthermore, binary



mixtures in which minor physical changes were observed, were also detected, and well separated by the PCA models. The optimal PCA model was obtained for the fingerprint region of the FTIR spectra, explaining 96.0 % of the spectral variation in the dataset, with good statistical indicators ( $R^2X = 0.960$  and  $Q^2 = 0.900$ ), as well as the PCA model for the DSC curves ( $R^2X = 0.981$  and  $Q^2 = 0.866$ ). The applied PLS-DA models have shown similar behavior as the PCA models, resulting in similar classification of the binary mixtures. In addition, the main spectral variations in the FTIR spectra, as well as the main thermal events in the DSC data were associated with the highest VIP scores in the corresponding VIP plots, confirming the model ability for predicting interactions. Furthermore, the predictive power of both PLS-DA models for FTIR spectra and DSC curves were evaluated and confirmed by the RMSEP value. The obtained RMSEP for the prediction set were 0.10 and 0.16 for the FTIR spectra model and DSC curve model, respectively, which demonstrates the capability of the optimized models for monitoring API-excipient compatibility during the preformulation testing. Based on PCA and PLS-DA results, it can be confirmed that multivariate analysis combined with FTIR spectroscopy and DSC analysis has great potential for compatibility studying and predicting of potential API-excipient interactions during pharmaceutical development. This is solid proof that machine learning is a powerful tool which can be further used for more detailed screening of API-excipient relations. Moreover, the continued adoption of AI and ML, beside the cost benefit, will unquestionably pave the future of the pharmaceutical industry, leading to even greater efficiency and productivity, faster product launch and increased chances of success in all areas of pharmaceutical development.

## 5. REFERENCES

- (1) Gupta, K. R.; Pounikar, A. R.; Umekar, M. J., Drug excipient compatibility testing protocols and characterization: a review. *Asian J. Chem. Sci.* **2019**, *6* (3), 1–22. <https://doi.org/10.9734/AJOCS/2019/v6i319000>
- (2) Rebiere, H.; Martin, M.; Ghyselinck, C.; Bonnet, P. A.; Brenier, C., Raman chemical imaging for spectroscopic screening and direct quantification of falsified drugs. *J. Pharm. Biomed. Anal.* **2018**, *148*, 316–323. <https://doi.org/10.1016/j.jpba.2017.10.005>
- (3) Hossain, M. N.; Igne, B.; Anderson, C. A.; Drennen III, J. K., Influence of moisture variation on the performance of Raman spectroscopy in quantitative pharmaceutical analyses. *J. Pharm. Biomed. Anal.* **2019**, *164*, 528–535. <https://doi.org/10.1016/j.jpba.2018.10.022>
- (4) Čapkova, T.; Pekárek, T.; Hanulíková, B.; Matějka, P., Application of reverse engineering in the field of pharmaceutical tablets using Raman mapping and chemometrics. *J. Pharm. Biomed. Anal.* **2022**, *209*, 114496. <https://doi.org/10.1016/j.jpba.2021.114496>
- (5) Antovska, P.; Petruševski, G.; Makreski, P., Solid-state compatibility screening of excipients suitable for development of indapamide sustained release solid-dosage formulation. *Pharm. Dev. Technol.* **2013**, *18* (2), 481–489. <https://doi.org/10.3109/10837450.2012.717948>
- (6) Chadha, R.; Bhandari, S., Drug-excipient compatibility screening – Role of thermoanalytical and spectroscopic techniques. *J. Pharm. Biomed. Anal.* **2014**, *87*, 82–97. <https://doi.org/10.1016/j.jpba.2013.06.016>
- (7) Selvaraj, C.; Chandra, I.; Singh, S. K., Artificial intelligence and machine learning approaches for drug design: challenges and opportunities for the pharmaceutical industries. *Mol. Diversity* **2021**, *23*, 1–21. <https://doi.org/10.1007/s11030-021-10326-z>
- (8) International Conference on Harmonisation of Technical Requirements for Registration of Pharmaceuticals for Human Use. ICH *Harmonised Tripartite Guideline on Pharmaceutical Development* Q8 (R2), European Medicines Agency, London, 2009.
- (9) Mansuri, N.; Patel, K.; Mehta, M.; Vyas, G.; Reddy, J. P.; Shah, T.; Steinbach, D.; Desai, D., Quality by design (QbD) approach to match tablet glossiness. *Pharm. Dev. Technol.* **2020**, *25* (8), 1010–1017. <https://doi.org/10.1080/10837450.2020.1772291>
- (10) Feng, H.; Mohan, S., Application of process analytical technology for pharmaceutical coating: challenges, pitfalls and trends. *AAPS PharmSciTech.* **2020**, *21*, 1–17. <https://doi.org/10.1208/s12249-020-01727-8>
- (11) *Guidance for industry: PAT – A framework for innovative pharmaceutical development, manufacturing and quality assurance*, U.S. Department of Health and Human Services, Food and Drug Administration, USA, 2004.
- (12) Lou, H.; Lian, B.; Hageman, M. J., Applications of machine learning in solid oral dosage form development. *J. Pharm. Sci.* **2021**, *110* (9), 3150–3165. <https://doi.org/10.1016/j.xphs.2021.04.013>
- (13) Patel, S.; Patel, M.; Kulkarni, M.; Patel, M. S., DE-INTERACT: A machine-learning-based predictive tool for the drug-excipient interaction study during product development – Validation through paracetamol and vanillin as a case study. *Int. J. Pharm.* **2023**, *637*, 122839. <https://doi.org/10.1016/j.ijpharm.2023.122839>
- (14) Wesolowski, M.; Rojek, B., Thermogravimetric detection of incompatibilities between atenolol and excipients using multivariate techniques. *J. Therm. Anal. Calorim.* **2013**, *113*, 169–177. <https://doi.org/10.1007/s10973-013-3070-y>
- (15) Rojek, B.; Wesolowski, M., A combined differential scanning calorimetry and thermogravimetry approach for the effective assessment of drug substance-excipient compatibility. *J. Therm. Anal. Calorim.* **2023**, *148* (3), 845–858. <https://doi.org/10.1007/s10973-022-11849-9>

- (16) Siozou, E.; Sakkas, V.; Kourkoumelis, N., Quantification and classification of diclofenac sodium content in dispersed commercially available tablets by attenuated total reflection infrared spectroscopy and multivariate data analysis. *Pharmaceuticals* **2021**, *14* (5), 440. <https://doi.org/10.3390/ph14050440>
- (17) Stojanovska Pecova, M.; Geskovski, N.; Petrushevski, G.; Chachorovska, M.; Krsteska, L.; Ugarkovic, S.; Makreski, P., Solid-state interaction of ibuprofen with magnesium stearate and product characterization thereof. *Drug Dev. Ind. Pharm.* **2020**, *46* (8), 1308–1317. <https://doi.org/10.1080/03639045.2020.1788067>
- (18) Talwar, S.; Pawar, P.; Wu, H.; Sowrirajan, K.; Wu, S.; Igne, B.; Friedman, R.; Muzzio, F. J.; Drennen III, J. K., NIR spectroscopy as an online PAT tool for a narrow therapeutic index drug: Toward a platform approach across lab and pilot scales for development of a powder blending monitoring method and endpoint determination. *AAPS PharmSciTech.* **2022**, *24* (6), 103. <https://doi.org/10.1208/s12248-022-00748-4>
- (19) Stojanovska Pecova, M.; Geskovski, N.; Petrushevski, G.; Makreski, P., A novel method for rapid particle size analysis of ibuprofen using near-infrared spectroscopy. *AAPS PharmSciTech.* **2021**, *22*, 1–13. <https://doi.org/10.1208/s12249-021-02156-x>
- (20) Company, A. D.; Simonetti, S., DFT study of the chemical reaction and physical properties of ibuprofen sodium. *Tetrahedron* **2022**, *120*, 132899. <https://doi.org/10.1016/j.tet.2022.132899>
- (21) Censi, R.; Martena, V.; Hoti, E.; Malaj, L.; Di Martino, P., Sodium ibuprofen dihydrate and anhydrous: study of the dehydration and hydration mechanisms. *J. Therm. Anal. Calorim.* **2013**, *111*, 2009–2018. <https://doi.org/10.1007/s10973-012-2194-9>
- (22) Rossi, P.; Macedi, E.; Paoli, P.; Bernazzani, L.; Carignani, E.; Borsacchi, S.; Geppi, M., Solid–solid transition between hydrated racemic compound and anhydrous conglomerate in Na-Ibuprofen: A combined X-ray diffraction, solid-state NMR, calorimetric, and computational study. *Cryst. Growth Des.* **2014**, *14* (5), 2441–2452. <https://doi.org/10.1021/cg500161e>
- (23) Chaïya, P. O.; Phaechamud, T. H., Differential scanning calorimetric analysis for incompatibility: sodium stearate/magnesium stearate and acidic compounds. *Key Eng. Mater.* **2020**, *859*, 307–312. <https://doi.org/10.4028/www.scientific.net/KEM.859.307>
- (24) Kararli, T. T.; Needham, T. E.; Seul, C. J.; Finnegan, P. M., Solid–state interaction of magnesium oxide and ibuprofen to form a salt. *Pharm. Res.* **1989**, *6*, 804–808. <https://doi.org/10.1023/A:1015983732667>
- (25) Ravichandran, V.; Lee, M.; Nguyen Cao, T.G.; Shim, M. S., Polysorbate-based drug formulations for brain-targeted drug delivery and anticancer therapy. *Appl. Sci.* **2021**, *11* (19), 9336. <https://doi.org/10.3390/app11199336>
- (26) Lombardo, R.; Musumeci, T.; Carbone, C.; Pignatello, R., Nanotechnologies for intranasal drug delivery: an update of literature. *Pharm. Dev. Technol.* **2021**, *26* (8), 824–845. <https://doi.org/10.1080/10837450.2021.1950186>
- (27) Kriegel, C.; Festag, M.; Kishore, R. S.; Roethlisberger, D.; Schmitt, G., Pediatric safety of polysorbates in drug formulations. *Children* **2019**, *7* (1), 1. <https://doi.org/10.3390/children7010001>
- (28) Garbacz, P.; Wesolowski, M., DSC, FTIR and Raman spectroscopy coupled with multivariate analysis in a study of co-crystals of pharmaceutical interest. *Molecules* **2018**, *23* (9), 2136. <https://doi.org/10.3390/molecules23092136>
- (29) Gao, Y.; Zhang, Y.; Hong, Y.; Wu, F.; Shen, L.; Wang, Y.; Lin, X., Multifunctional role of silica in pharmaceutical formulations. *AAPS PharmSciTech.* **2022**, *23* (4), 90. <https://doi.org/10.1208/s12249-022-02237-5>
- (30) Rojek, B.; Gazda, M.; Wesolowski, M., Quantification of compatibility between polymeric excipients and atenolol using principal component analysis and hierarchical cluster analysis. *AAPS PharmSciTech.* **2022**, *23*, 1–16. <https://doi.org/10.1208/s12249-021-02143-2>
- (31) Lasalvia, M.; Capozzi, V.; Perna, G., A comparison of PCA-LDA and PLS-DA techniques for classification of vibrational spectra. *Appl. Sci.* **2022**, *12* (11), 5345. <https://doi.org/10.3390/app12115345>